*Proc. Natl. Acad. Sci. USA*
Vol. 95, pp. 8785–8790, July 1998
Immunology

# Activation of preexisting T cell clones by targeted interleukin 2 therapy

PER THOR STRATEN*, PER GULDBERG*, TINA SEREMET*, RALPH A. REISFELD†‡, JESPER ZEUTHEN*, AND JÜRGEN C. BECKER§

*Department of Tumor Cell Biology, Division of Cancer Biology, Danish Cancer Society, DK-2100 Copenhagen, Denmark; †Department of Immunology, Scripps Research Institute, La Jolla, CA 92037; and §Department of Dermatology, School of Medicine, D-97080 Würzburg, Germany

*Communicated by Frank J. Dixon, Scripps Research Institute, La Jolla, CA, April 30, 1998 (received for review February 19, 1998)*

**ABSTRACT** **The induction of an immunological antitumor response capable of eradicating metastatic tumors is the ultimate goal of immunotherapy. We have recently shown that this can be achieved by interleukin 2 (IL-2) therapy directed to the tumor microenvironment by a recombinant antibody–IL-2 fusion protein. It is not known, however, whether this curative treatment is associated with a predominance of T cells carrying specific T cell receptor variable β regions (TCRBV) or the presence of clonally expanded T cells. To address this question, we have used a quantitative reverse transcriptase-coupled PCR method to analyze the TCRBV region repertoire in tumor-infiltrating lymphocytes of treated and untreated animals. As controls the TCRBV region repertoire was analyzed in blood and skin from disease-free animals. The results indicate an overexpression of TCRBV5 in the tumors of all treated mice and an additional overexpression of individual regions in each tumor. Direct sequencing of these TCRBV regions did not reveal any evidence of clonal expansions. However, since clonal expansions could exist as subpopulations in highly expressed regions, not detectable by direct sequencing, a denaturing gradient gel electrophoresis assay was used for clonal analysis of TCRBV PCR products. Denaturing gradient gel electrophoresis analysis of selected TCRBV regions revealed the presence of clonotypic T cells in tumors from both treated and untreated animals. These data indicate that targeted IL-2 therapy in this model does not induce clonal T cell responses *de novo*, rather it acts as an activator for an already existing population of clonotypic T cells.**

Melanoma is a highly malignant tumor but several lines of evidence suggest that it is capable of eliciting a specific immune response, i.e., a number of melanoma-associated antigens have been identified and the presence of clonotypic T cells has been demonstrated in melanoma lesions (1–4). Therefore, several immunomodulatory therapeutic approaches were initiated to improve the prognosis of melanoma patients. Interleukin 2 (IL-2) is one of the most potent antitumor cytokines known quote (5), and was recently approved for treatment of metastatic melanoma. However, objective responses induced by systemic IL-2 therapy are still insufficient, and the associated side effects are severe (6). These findings are due to the fact that a systemic application of IL-2 disregards the paracrine nature of this cytokine under physiological conditions (7).

As a means to target IL-2 directly to the tumor site, we have recently shown that human IL-2 can be genetically engineered as a fusion protein with the chimeric mouse–human mAb 14.18 which recognizes the ganglioside $GD_2$, retaining both antigen binding and cytokine activity (8). Furthermore, we have shown that treatment with this antibody–IL-2 fusion protein can eradicate human hepatic and pulmonary melanoma metastases in severe combined immunodeficient mice (9) as well as autologous murine B16 melanomas (10). Although it was shown in these studies that tumor eradication was dependent on $CD8^+$ T cells, it is not known whether tumor clearance is associated with a clonal expansion of T cells. Furthermore, it remains to be established whether such a clonal expansion would be due to a *de novo* induction or to the activation and expansion of preexisting T cell clones. Here, we demonstrate both the overexpression of certain T cell receptor variable β regions (TCRBV) as well as the clonal expansion of T cells in melanoma lesions subsequent to targeted IL-2 therapy. However, clonally expanded T cells were also detectable prior to therapy, suggesting that antibody–IL-2-targeted therapy acts as an activator rather than an inducer of an antitumor T cell response.

## MATERIALS AND METHODS

**Cell Lines, Antibodies, and Fusion Proteins.** The murine melanoma cell lines B16 G.3.12 and B78-D14 have been described previously (8). B78-D14 was derived from B16 melanoma cells by transfection with genes coding for β-1,4-*N*-acetylgalactosaminyltransferase and α-2,8-sialyltransferase inducing a constitutive expression of the gangliosides GD2 and GD3. B16 melanoma cells were maintained as monolayers in RPMI 1640 medium supplemented with 10% fetal calf serum and 2 mM L-glutamine and were passaged as necessary. The culture medium for B78-D14 cells was further supplemented with 400 μg of G418 and 50 μg of Hygromycin B/μl.

Mouse/human chimeric antibodies directed against the epidermal growth factor receptor (ch225) or GD2 (ch14.18) were constructed by joining the cDNA for the variable region of the murine antibodies with the constant regions of the γ1 heavy chain and the κ light chain as described previously (9). The antibody–IL-2 fusion proteins ch225–IL-2 and ch14.18–IL-2 were constructed by fusion of a synthetic sequence coding for human IL-2 to the carboxyl end of the human Cγ1 gene as described (5, 10). The fused genes were inserted into the vector pdHL2 which encodes for the dihydrofolate reductase gene (10). The resulting expression plasmids were introduced into Sp2/0-Ag14 cells and selected in DMEM supplemented with 10% fetal bovine serum and 100 nM methotrexate. The fusion proteins were purified over a protein A–Sepharose affinity column.

All other antibodies used are commercially available and have been described in detail by the manufacturer (PharMingen).

The publication costs of this article were defrayed in part by page charge payment. This article must therefore be hereby marked "*advertisement*" in accordance with 18 U.S.C. §1734 solely to indicate this fact.



Abbreviations: DGGE, denaturing gradient gel electrophoresis; IL-2, interleukin 2; TCR, T cell receptor; BV, β variable region; RT, reverse transcription; PBL, peripheral blood lymphocyte.

‡To whom reprint requests should be addressed at: Department of Immunology, Scripps Research Institute, IMM 13, R218, 10550 North Torrey Pines Road, La Jolla, CA 92037.

**Animals.** C57BL/6J mice were obtained from The Jackson Laboratory at the age of 4–6 wk. These animals were housed under specific pathogen-free conditions and all experiments were performed according to the National Institutes of Health Guidelines for Care and Use of Laboratory Animals.

**s.c. Tumors.** Tumors were induced by s.c. injection of $5 \times 10^6$ tumor cells in RPMI 1640, which resulted in tumors of approximately 40-$\mu$l volume within 14 days.

**Immunohistology.** Frozen sections were fixed in cold acetone for 10 min followed by removal of endogenous peroxidase with 0.03% $H_2O_2$ and blocking of collagenous elements with 10% species-specific serum in 1% BSA/PBS. The antibodies where then overlayed onto serial sections, at predetermined dilutions (usually 20 $\mu$g/ml), and the slides were incubated in a humid chamber for 30 min. With PBS washes between every step, a biotinylated link antibody was applied for 10 min followed by a streptavidin-linked enzyme, i.e., either peroxidase or alkaline phosphatase, for 10 min. After another wash, the substrate was added and the slides were incubated in the dark for 20 min. After a wash in PBS, the slides were counter stained, mounted, and viewed using an Olympus BH2 microscope with photographic capabilities.

**RNA Extraction and cDNA Synthesis.** RNA was extracted using the method of Chomczynski and Sacchi as described (11, 12). cDNA synthesis was carried out using 1–3 $\mu$g of total RNA with oligo-dT and M-MLV SuperScript II reverse transcriptase (GIBCO/BRL) in a total volume of 50 $\mu$l of 1× buffer (GIBCO/BRL) containing 10 mM DTT. Incubations were performed at 42°C for 50 min and at 72°C for 5 min.

**Primer Design and Characteristics.** Primers used for the amplification of murine TCR regions include 18 primers specific for $\beta$ variable region (TCRBV) families 1–18 and primers specific for the $\beta$ constant region primer, TCRBC (Table 1). Murine TCRBV sequences in the GenBank database (13) were used in combination with the PCGENE FASTSCAN program (Intelligenetics, Palo Alto, CA) to create library files for the BV families 1–18. Optimal primer sequences were found by using the computer program Oligo Version 3.4 (Medprobe, Oslo, Norway) (14) aiming at a $\Delta G$ below $-40.0$ and a $T_m$ between 50 and 60°C. Selected primer sequences were tested for match to all members of the respective families. Importantly, all sequences were subsequently tested for potential homology to all other families, aiming at a minimum of five mismatches to nonrelevant templates. All primers fulfill these criteria.

**TCRBV Analysis and Quantitation.** Preliminary experiments were performed to certify that TCRBV analyses were performed in the exponential phase of the amplification, ensuring a proportional relationship between the amount of mRNA in the original sample and the amount of PCR product. cDNA was serially diluted (2-fold dilutions down to 1/512) and PCR amplified for 26 cycles with TCRBC-specific primers (BC-5 and BC-3). The amount of TCRBC PCR product was quantitated using Imagequant software (15) and these results were used to ensure that all TCRBV analyses were carried out using an equal amount of T cell receptor (TCR) cDNA. Amplifications were performed twice in a total volume of 25 $\mu$l containing 5 pmol of each primer, 2.5 mM 2′-deoxynucleoside 5′triphosphates (Pharmacia LKB), and 1.25 units of Amplitaq polymerase (Perkin–Elmer/Cetus) in 1× PCR buffer [50 mM KCl, 20 mM Tris (pH 8.4), 2.0 mM $MgCl_2$, 0.2 mM cresol, 12% sucrose, and 0.005% (wt/vol) BSA (Boehringer Mannheim)]. Inclusion of sucrose and cresol red in the reaction buffer enables direct loading of aliquots on the gel (16). Negative controls were samples without cDNA. TCRBV amplifications were performed by 30 cycles in a Perkin–Elmer GeneAmp PCR System 9600 (Perkin–Elmer/Cetus) using the following parameters: 94°C for 30 sec, 60°C for 30 sec, and 72°C for 60 sec. *Taq* polymerase and 2′-deoxynucleoside 5′-triphosphates were added to the reaction at an 80°C step between the denaturation and annealing steps of the first cycle (hot start) (17). For quantitative PCR analysis the constant region primer (BC) was end labeled with [$\gamma$-$^{33}$P]. Ten-microliter aliquots of PCR products were electrophoresed in a 2% NuSieve 3:1 agarose gel (FMC), which was subsequently dried under vacuum and exposed to a Molecular Dynamics Storage Phosphor Screen (Molecular Dynamics). Quantitation was accomplished using the Imagequant software (15).

**Denaturing Gradient Gel Electrophoresis (DGGE).** Melting maps were generated using the computer algorithm MELT87

Table 1. Primers used for the amplification of variable (BV) and constant (BC) regions of the $\beta$ chain of the murine TCR

| | | $\Delta G$ | $T_m$, °C | Position | Size, bp |
|---|---|---|---|---|---|
| BV1 | 5′-CGGTGCCCAGTCGTTTTATAC-3′ | −40.8 | 53.8 | −89 | 223 |
| BV2 | 5′-CACACGGGTCACTGATACGGAG-3′ | −41.0 | 56.7 | −61 | 195 |
| BV3 | 5′-CACCTTGCAGCCTAGAAATTCAG-3′ | −42.5 | 54.9 | −50 | 184 |
| BV4 | 5′-CTGCCTCAAGTCGCTTCCAAC-3′ | −41.2 | 56.3 | −89 | 223 |
| BV5 | 5′-TGARATGAACATGAGTGCCTTGG-3′ | −41.3 | 56.4 | −43 | 177 |
| BV6 | 5′-TTCTCTCACTGTGACATCTGCCC-3′ | −40.1 | 56.5 | −42 | 176 |
| BV7 | 5′-AAGGATACAGGGTCTCACGGAAG-3′ | −42.7 | 55.3 | −80 | 214 |
| BV8 | 5′-GATRTCCCTGATGGRTACAAGGC-3′ | −43.9 | 58.3 | −40 | 174 |
| BV8A | 5′-TTGGCTTCCCTCTCTCAGACA-3′ | −39.2 | 53.8 | −27 | 161 |
| BV9 | 5′-TCTCTCTACATTGGCTCTGCAGG-3′ | −44.7 | 58.7 | −42 | 176 |
| BV10 | 5′-ATCAAGTCTGTAGAGCCGGAGG-3′ | −41.1 | 54.1 | −33 | 167 |
| BV11 | 5′-AGGCACAAGGTGACAGGGAAG-3′ | −40.4 | 55.5 | −243 | 377 |
| BV12 | 5′-ATGGTGGGGCTTTCAAGGATC-3′ | −42.3 | 56.6 | −98 | 232 |
| BV13 | 5′-CTGTGAGGCCTAAAGGAACTAAC-3′ | −40.7 | 51.1 | −68 | 202 |
| BV14 | 5′-ACGACCAATTCATCCTAAGCAC-3′ | −40.1 | 52.5 | −53 | 187 |
| BV15 | 5′-CCATCAGTCATCCCAACTTATCC-3′ | −41.4 | 54.0 | −69 | 203 |
| BV16 | 5′-GTGACCCTCAATTGTGACCCAG-3′ | −40.4 | 55.6 | −213 | 347 |
| BV17 | 5′-CACGATACCTGGTCAAAGAGAAAG-3′ | −42.2 | 53.9 | −245 | 379 |
| BV18 | 5′-CGGCCAAACCTAACATTCTC-3′ | −41.9 | 55.1 | −63 | 215 |
| BC | 5′-GGGTAGCCTTTTGTTTGTTTGC-3′ | −42.5 | 54.6 | 84 | |
| BC-5′ | 5′-GCTACCTTCTGGCACAATCCTC-3′ | −41.2 | 54.5 | 236 | |
| BC-3′ | 5′-TAGGCATTTTCCAGGTCACAAG-3′ | −40.6 | 53.5 | 699 | 463 |
| | GC clamp: 5′-CGCCCGCCGCGCCCCGCGCCCGTCCCGCCGCCCCCGCCC-3′ | | | | |

Position +1 is defined as the first nucleotide 5′ to the sequence coding for the conserved amino acid sequence CASS in the proximal end of the variable region. The approximate size is calculated using an estimated length of the DJ region of 50 bp.

(18). DGGE analyses were done in 6% polyacrylamide gels containing a gradient of urea and formamide from 20 to 80% (19). Electrophoresis was performed at 160 V for 4.5 hr in 1× TAE buffer at a constant temperature of 58°C. After electrophoresis, the gels were stained with ethidium bromide and photographed under UV transillumination. To validate the resolving power of the method, BV regions selected for clonal analysis were cloned using the TA cloning kit following the manufacturer's suggestions (Invitrogen). Positive bacterial clones were PCR amplified for 35 cycles with the specific BV primer along with the "GC-clamped" BC primer, and 12-$\mu$l aliquots were analyzed using DGGE.

**Sequencing Reaction.** Several PCR products were subjected to sequence analysis to investigate the clonality of the transcript using the Thermo Sequenase cycle sequencing kit (Amersham) according to the manufacturer's instructions. In brief, bands were excised from the denaturing gradient gel, and DNA was eluted in $H_2O$ and reamplified. An aliquot (0.2 $\mu$l) of the PCR product was used as template in a 40-cycle sequencing reaction with [$\gamma$-$^{33}$P] end-labeled BC as sequencing primer. Gels were dried under vacuum and exposed to a Phosphor Screen.

## RESULTS

**Quantitative Reverse Transcriptase–PCR of TCRBV Regions.** The tumors used for investigation were induced by s.c injection of either the parental B16 melanoma line G3.12 (20) or the GD2-expressing melanoma line B78-D14 derived from the B16 melanoma cells by transfection with genes coding for $\beta$-1,4-*N*-acetylgalactosaminyltransferase and $\alpha$-2,8-sialyltransferase (21). Tumors were obtained from mice which were treated by i.v. administration of 8 $\mu$g of ch14.18–IL-2 fusion protein for 7 days. Therapy was initiated 10 days after tumor cell inoculation. As controls, we used tumor samples obtained from mice receiving PBS instead of ch14.18–IL-2. To analyze for the expression of TCRBV region expression in murine blood, skin, and tumor tissues, we have designed 18 primers specific for murine TCRBV families 1–18. Prior to analysis of tumor lesions, experiments were carried out to demonstrate that each amplified TCRBV product was obtained with the expected size (see Table 1) and no spurious amplification products were observed. To validate the semiquantitative reverse transcriptase–PCR methodology, serially diluted cDNA was PCR amplified for different numbers of cycles (26, 28, 30, 32, and 34 cycles) using the primers BV 1–18 in combination with the constant region primer BC end labeled with [$\gamma$-$^{33}$P]. The data from these experiments (data not shown) were used to determine the amount of cDNA and the number of cycles through which the specific PCR products accumulated exponentially, enabling determination of the relative abundance of each TCRBV region. Furthermore, the accuracy and reproducibility of the method were investigated by repeated analyses of peripheral blood lymphocytes (PBLs), indicating that the experimental variation represented 4–8% of the mean value. The relative expressions of TCRBV regions in different tumors are shown in Table 2. The expression of each TCRBV family is given as the mean percentage (±SD) of the total TCRBV signal detected in the gel. As additional controls we analyzed the TCRBV1–18 expression in PBLs and skin from four healthy animals. Results from these analyses are shown in Table 3.

In general, all analyses showed low expression of TCRBV17 and 18 and high expression of TCRBV8. One possible explanation for this observation is that most murine BV families are single-member families whereas BV8 is a three-member family. A comparison of $GD_2$-expressing tumors in treated versus untreated animals indicates a significantly higher expression of BV5 in animals treated with the fusion protein (Table 2). The mean expression of BV5 in tumors derived from the untreated animals was 5.6%, whereas it was 17.1% in tumors of animals treated with ch14.18–IL-2. In several tumors, one or two additional BV families were expressed at levels ≥10%. This high expression was observed with the families BV1, 6, 11, 12, and 13. Like BV5, the high expression of BV12 is observed in several B16 G3.12 tumors as well as B78-D14 tumors from both treated and untreated mice.

**DGGE.** To investigate the clonality of the transcripts, several PCR products from tumor tissues were sequenced directly through the CDR3-coding region of the receptor. A total of 21 different PCR products were sequenced, including BV5 from all 12 animals; BV8, BV11, and BV13 from animal 1 of the B16 G3.12 fusion protein group; BV1 and BV8 from animal 1; and BV8 and BV12 from animal 3 of the B78–D14 fusion protein group. These experiments revealed no indications of clonality. For a correct interpretation of this finding, it is important to

Table 2. Relative expression of TCRBV regions 1-18 in B16 G3.12 and B78–D14 tumors in PBS-treated animals as well as B78–D14 tumors in ch14.18–IL-2-treated animals

| | B16/7 days of PBS | | | | B16/$DG_2$/7 days of PBS | | | | B16/$DG_2$/7 days of ch14.18–IL-2 | | | |
|---|---|---|---|---|---|---|---|---|---|---|---|---|
| | Animal 1 % (SD) | Animal 2 % (SD) | Animal 3 % (SD) | Animal 4 % (SD) | Animal 1 % (SD) | Animal 2 % (SD) | Animal 3 % (SD) | Animal 4 % (SD) | Animal 1 % (SD) | Animal 2 % (SD) | Animal 3 % (SD) | Animal 4 % (SD) |
| BV1 | 5.4 (0.4) | 4.9 (1.4) | 11.3 (ND) | 5.2 (0.7) | 10.9 (0.7) | 2.8 (1.5) | 9.4 (5.2) | 4.3 (0.9) | 6.1 (0.1) | 3.4 (0.2) | 4.4 (0.4) | 6.8 (2.2) |
| BV2 | 4.2 (0.9) | 5.1 (1.8) | 4.1 (ND) | 5.9 (1.8) | 5.4 (0.7) | 7.2 (1.9) | 4.4 (1.7) | 6.1 (0.3) | 5.4 (0.6) | 6.5 (1.1) | 4.7 (0.7) | 7.1 (0.4) |
| BV3 | 5.7 (0.5) | 4.9 (1.4) | 1.2 (ND) | 2.7 (1.1) | 2.9 (0.2) | 3.6 (1.0) | 4.0 (0.6) | 2.6 (0.3) | 2.5 (0.6) | 1.4 (0.6) | 2.7 (0.5) | 4.5 (0.9) |
| BV4 | 1.6 (0.6) | 4.2 (0.1) | 2.5 (ND) | 2.1 (0.5) | 3.4 (0.0) | 6.8 (3.2) | 2.2 (0.2) | 3.3 (0.3) | 2.1 (0.6) | 1.4 (0.1) | 2.2 (0.1) | 2.7 (1.3) |
| BV5 | 8.1 (0.6) | 6.2 (0.3) | 5.9 (ND) | 7.7 (2.3) | 4.7 (0.4) | 6.2 (1.3) | 5.2 (0.6) | 6.3 (1.7) | 11.6 (2.4) | 28.8 (1.2) | 17.5 (0.6) | 10.3 (1.4) |
| BV6 | 12.7 (0.4) | 6.4 (1.3) | 19.9 (ND) | 5.0 (0.1) | 5.2 (1.7) | 3.9 (0.4) | 5.9 (0.8) | 5.4 (0.8) | 6.9 (0.4) | 5.2 (0.8) | 4.1 (0.1) | 5.1 (0.3) |
| BV7 | 3.7 (1.2) | 4.3 (0.6) | 2.3 (ND) | 3.5 (1.9) | 2.9 (0.8) | 2.8 (0.8) | 3.4 (0.8) | 3.6 (0.3) | 6.0 (1.1) | 4.6 (1.1) | 6.8 (1.4) | 5.8 (0.2) |
| BV8 | 13.2 (0.2) | 5.3 (0.2) | 10.5 (ND) | 18.9 (1.7) | 30.4 (4.0) | 10.1 (0.7) | 22.7 (1.1) | 14.9 (1.4) | 18.2 (0.4) | 16.8 (0.5) | 17.7 (0.7) | 9.3 (3.1) |
| BV9 | 4.0 (1.2) | 4.3 (1.3) | 1.6 (ND) | 3.7 (1.1) | 4.0 (0.7) | 3.0 (0.7) | 6.0 (0.6) | 3.7 (0.1) | 5.8 (0.1) | 3.8 (0.1) | 3.3 (1.2) | 5.2 (0.4) |
| BV10 | 3.1 (0.8) | 7.4 (0.3) | 3.1 (ND) | 4.8 (0.3) | 4.0 (0.1) | 6.1 (0.3) | 6.0 (1.0) | 6.2 (0.6) | 5.4 (1.1) | 4.8 (1.3) | 7.8 (0.5) | 6.1 (0.6) |
| BV11 | 11.5 (2.6) | 5.7 (0.1) | 12.6 (ND) | 9.0 (3.1) | 7.1 (1.2) | 5.4 (0.6) | 2.5 (0.4) | 5.4 (0.2) | 5.2 (0.9) | 6.1 (0.1) | 4.7 (0.8) | 5.3 (1.8) |
| BV12 | 5.8 (0.7) | 8.4 (1.3) | 10.8 (ND) | 6.2 (0.0) | 3.5 (1.3) | 12.9 (0.5) | 5.9 (1.0) | 15.5 (0.0) | 7.5 (1.9) | 6.7 (1.6) | 10.5 (0.6) | 7.7 (1.1) |
| BV13 | 9.9 (4.0) | 10.2 (1.4) | 3.4 (ND) | 5.1 (1.2) | 2.3 (0.3) | 4.4 (0.5) | 3.3 (0.0) | 4.7 (0.3) | 6.5 (1.5) | 3.8 (1.3) | 4.1 (0.8) | 6.8 (0.2) |
| BV14 | 2.8 (1.3) | 7.5 (2.1) | 2.4 (ND) | 3.0 (0.1) | 2.5 (0.5) | 9.8 (0.2) | 4.5 (0.7) | 3.8 (1.0) | 2.5 (0.0) | 2.3 (0.5) | 3.2 (0.3) | 5.7 (0.4) |
| BV15 | 3.8 (1.0) | 5.0 (1.0) | 2.2 (ND) | 4.5 (0.2) | 5.0 (0.1) | 6.6 (0.1) | 9.3 (0.4) | 6.2 (0.0) | 2.0 (0.0) | 1.4 (0.5) | 2.1 (0.3) | 4.5 (0.3) |
| BV16 | 3.9 (0.2) | 5.9 (1.8) | 4.6 (ND) | 6.4 (0.8) | 5.0 (0.2) | 7.2 (1.0) | 4.6 (0.9) | 7.3 (2.3) | 5.1 (0.1) | 2.8 (0.2) | 3.6 (0.4) | 4.5 (0.3) |
| BV17 | 0.2 (0.1) | 1.1 (0.9) | 0.7 (ND) | 0.4 (0.2) | 0.1 (0.0) | 0.3 (0.0) | 0.4 (0.1) | 0.1 (0.0) | 0.5 (0.1) | 0.3 (0.1) | 0.4 (0.4) | 0.2 (0.0) |
| BV18 | 0.4 (0.2) | 3.3 (0.0) | 0.5 (ND) | 5.7 (0.9) | 0.7 (0.1) | 0.9 (0.7) | 0.1 (0.1) | 0.4 (0.0) | 0.7 (0.4) | 0.2 (0.1) | 0.2 (0.1) | 0.4 (0.1) |

The expression of each BV region was calculated as a percentage of the sum of all BV spots.

Table 3. TCRBV 1-18 expression in PBLs and skin from untreated animals.

| | Animal 1 | | Animal 2 | | Animal 3 | | Animal 4 | |
|---|---|---|---|---|---|---|---|---|
| | PBLs % (SD) | Skin % (SD) | PBLs % (SD) | Skin % (SD) | PBLs % (SD) | Skin % (SD) | PBLs % (SD) | Skin % (SD) |
| BV1 | 3.7 (1.1) | 5.5 (0.7) | 4.1 (0.0) | 2.6 (1.0) | 6.2 (1.0) | 6.2 (0.8) | 6.2 (1.0) | 10.5 (2.1) |
| BV2 | 6.7 (0.8) | 7.4 (0.1) | 8.4 (1.8) | 8.0 (1.3) | 5.5 (0.0) | 7.0 (0.7) | 5.5 (0.0) | 7.4 (2.4) |
| BV3 | 2.6 (0.2) | 3.7 (1.0) | 4.3 (0.8) | 2.2 (0.7) | 3.2 (0.0) | 3.0 (0.4) | 3.2 (0.0) | 4.1 (1.2) |
| BV4 | 1.2 (0.8) | 2.2 (0.4) | 1.3 (0.0) | 2.2 (0.3) | 4.1 (0.3) | 1.8 (0.9) | 4.1 (0.3) | 1.6 (0.4) |
| BV5 | 5.8 (0.3) | 10.3 (1.2) | 9.7 (0.5) | 5.9 (0.5) | 7.6 (2.2) | 9.1 (0.9) | 7.6 (2.2) | 9.5 (0.0) |
| BV6 | 6.0 (2.3) | 6.0 (0.1) | 9.2 (4.1) | 19.5 (0.6) | 7.3 (0.2) | 5.8 (0.7) | 7.3 (0.2) | 5.1 (0.9) |
| BV7 | 7.8 (1.3) | 4.5 (1.2) | 3.4 (1.8) | 5.1 (0.3) | 4.4 (0.7) | 2.5 (1.1) | 4.4 (0.7) | 4.1 (0.3) |
| BV8 | 24.2 (3.8) | 14.0 (3.0) | 15.6 (2.2) | 16.0 (0.0) | 11.8 (2.0) | 12.0 (5.3) | 11.9 (2.0) | 13.0 (1.1) |
| BV9 | 3.6 (0.1) | 4.3 (0.2) | 5.3 (1.0) | 3.9 (1.5) | 3.8 (0.5) | 4.0 (1.4) | 3.8 (0.5) | 2.9 (1.3) |
| BV10 | 4.7 (0.1) | 5.8 (0.8) | 8.9 (1.4) | 6.7 (1.4) | 7.9 (1.8) | 4.9 (2.4) | 7.9 (1.8) | 6.5 (0.2) |
| BV11 | 2.7 (0.3) | 4.9 (0.6) | 1.6 (1.4) | 5.3 (1.0) | 4.0 (1.0) | 1.7 (0.3) | 4.0 (1.0) | 2.9 (0.5) |
| BV12 | 5.9 (0.7) | 9.5 (0.0) | 8.2 (3.0) | 2.1 (1.1) | 8.4 (1.3) | 20.0 (2.6) | 8.4 (1.3) | 8.5 (0.5) |
| BV13 | 4.1 (0.3) | 5.0 (0.2) | 4.9 (1.1) | 9.2 (1.8) | 7.1 (0.1) | 6.1 (0.5) | 7.1 (0.1) | 7.7 (1.5) |
| BV14 | 5.5 (0.4) | 4.9 (1.1) | 8.1 (0.6) | 4.0 (1.4) | 7.6 (1.2) | 5.8 (0.9) | 7.6 (1.2) | 6.0 (0.9) |
| BV15 | 3.3 (0.1) | 4.2 (0.4) | 3.4 (2.2) | 1.6 (0.6) | 3.2 (0.4) | 4.8 (1.4) | 3.2 (0.4) | 3.0 (0.3) |
| BV16 | 12.0 (0.7) | 7.2 (0.6) | 2.6 (1.7) | 2.8 (0.2) | 7.0 (0.0) | 3.3 (0.1) | 7.0 (0.0) | 4.8 (0.3) |
| BV17 | 0.1 (0.1) | 0.1 (0.1) | 0.4 (0.0) | 1.2 (1.0) | 0.4 (0.1) | 1.1 (0.1) | 0.4 (0.1) | 0.9 (0.5) |
| BV18 | 0.1 (0.1) | 0.4 (0.0) | 0.3 (0.3) | 0.3 (0.1) | 0.4 (0.0) | 0.9 (0.7) | 0.4 (0.0) | 1.2 (1.1) |

The expression of each BV region was calculated as a percentage of the sum of all BV spots.

point out that clonally expanded T cells must account for at least 10% of the T cell infiltrate to be detected by direct sequencing. Thus, we applied the DGGE methodology to resolve whether clonal T cells might be present in the T cell infiltrate at lower frequencies.

The melting properties of several TCRBV5, BV8, and BV12 sequences available were evaluated by use of the computer program MELT 87 which predicts the melting of a double-stranded DNA molecule on the basis of its base composition (13, 18). These calculations indicated that the DNA molecules amplified by the BV5 and BV12 primers were suited for denaturing gradient gel analysis, whereas the BV8 primer had to be changed (BV8A; Table 1). The subsequent attachment of a GC-rich sequence (GC clamp) to the 5′ end of the constant region (Table 1) altered the melting profile of all tested sequences to generate the desired two-domain profile (22). To validate the resolving power of the method, cloned transcripts derived from TCRBV5, 8, and 12 were analyzed. In all cases clonal PCR products were resolved as distinct bands in the gel, whereas analysis of polyclonal products revealed a smear (Fig. 1). At least eight different clonotypic transcripts were analyzed for each of the BV regions (BV5, 8, and 12), and in all cases the products resolved at different positions in the gel (Fig. 1 and data not shown).

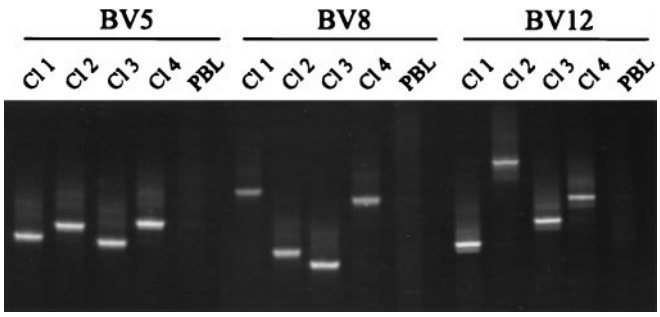


FIG. 1. Denaturing gradient gel analysis of polyclonal (PBLs) and clonal TCR transcripts covering BV5, BV8, and BV12. cDNA from PBLs was amplified with primers specific for BV families 5, 8, or 12, cloned into PCR (Invitrogen), and reamplified. PCR products were loaded onto a 20–80% denaturing gradient gel and run for 4.5 hr at 160 V at a constant temperature of 58°C. DNA was stained with ethidium bromide and photographed under UV light.

Following this validation, we tested for the presence of clonotypic T cells in different tumor samples. Tumor-infiltrating lymphocytes from three groups, i.e., B16 G3.12 and B78-D14 tumors in PBS-treated animals as well as B78-D14 tumors in ch14.18–IL-2 fusion protein-treated animals were analyzed by DGGE for the presence of T cell clonality in BV families 5, 8, and 12. Skin and PBLs from four disease-free animals were analyzed as controls. Clonotypic transcripts were revealed in all tumors for at least one of the regions analyzed (see Fig. 3). In contrast, for skin and PBL samples in only one single case (skin sample 3), a clonal BV12 transcript could be detected (Fig. 2). Multiple DNA bands were recovered from the gels, reamplified, and sequenced in all cases, verifying the clonality of the transcript. As shown in Fig. 3, DGGE analysis demonstrated the presence of clonally expanded T cells in B78-D14 tumors of animals receiving either ch14.18–IL-2 or PBS. Furthermore, clonally expanded T cells were also present in GD2-negative B16 G3.12 tumors; thus, demonstrating the immunogenicity of the parental B16 line. In most lesions more than one clonal transcript was detected, and in some lesions several clonal transcripts were found that carried the same BV region.

## DISCUSSION

The past decade has unveiled important insights into the role of T lymphocytes in the host's immune response to cancer in general and to melanoma in particular (1). A number of

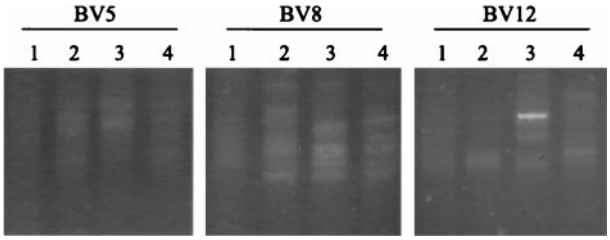


FIG. 2. Denaturing gradient gel analysis of skin from healthy animals. BV5, BV8, and BV12 transcripts were amplified from skin cDNA. Ten-microliter aliquots were loaded onto a 20–80% denaturing gradient gel and run for 4.5 hr at 160 V at a constant temperature of 58°C. DNA was stained with ethidium bromide and photographed under UV light.

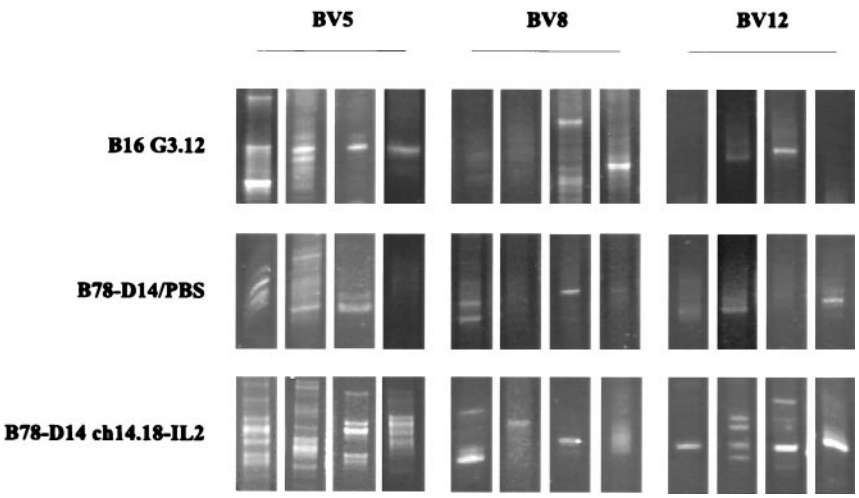


FIG. 3. Denaturing gradient gel analysis for clonality in tumor-infiltrating lymphocytes in B16 G3.12, B78–D14/PBS, and B78–D14 ch14.18–IL-2. From four animals in each group (left to right) cDNA from tumor biopsies were PCR amplified with primers specific for BV5, BV8, and BV12 along with the GC-clamped constant regions primer. Aliquots were loaded onto a 20–80% denaturing gradient gel and run for 4.5 hr at 160 V at a constant temperature of 58°C. DNA was stained with ethidium bromide and photographed under UV light.

tumor-associated antigens have been characterized which are specifically recognized by autologous T cells in the context of HLA molecules (23).The notion that a functional and specific T cell response is present in melanoma patients is corroborated by the observation that clonotypic T cells exist in both primary and metastatic melanoma (4, 24). However, the unfavorable prognosis of metastatic melanoma clearly demonstrates that this immunological response is inadequate to eradicate the tumor.

IL-2, which has a central role in the immune system, has been widely used for the treatment of metastatic melanoma (25). However, the systemic administration of this cytokine disregards its paracrine nature, thus resulting in limited antitumor responses and severe side effects (6). Recently, we have tried to overcome these problems by developing antibody–IL-2 fusion proteins that combine the unique targeting ability of antibodies with the multifunctional activity of cytokines. The therapeutic effectiveness of such constructs for the treatment of established hepatic, pulmonary, and subcutaneous melanoma metastases has been documented in a number of different murine tumor models (9, 10, 26–28). Detailed characterization in various tumor models revealed the superiority of antibody–IL-2 fusion proteins over comparable amounts of IL-2, the parental antibody, the combination of both or nonspecific antibody–IL-2 fusion proteins (9). Even micrometastases displaying some degree of antigenic heterogeneity could be successfully addressed by this form of therapy. Several lines of evidence, i.e., immunohistology, *in vivo* depletion studies, adoptive transfer experiments, and cytotoxicity assays, indicated that this antitumor effect is largely dependent on $CD8^+$ T cells (29). However, the molecular basis of this T cell response remained elusive.

In the present study, we scrutinized the nature of the T cell response at the molecular level. Our aim was to test whether specific TCRBV regions were overexpressed in the T cell infiltrate of tumors before and after targeted immunotherapy, followed by an analysis of these regions for clonality. The quantitative analysis of TCRBV1–18 in three groups of tumor samples, i.e., B16 G3.12, and B78-D14 tumors in PBS-treated animals, as well as B78–D14 tumors in ch14.18–IL-2 fusion protein-treated animals, revealed an overexpression of BV5 in B78–D14 tumors after therapy with ch14.18–IL-2 (Table 2). However, since the expression of BV5 was rather high in a limited number of skin samples (Table 3), it was not prudent to conclude that this overexpression was due to a clonal expansion of T cell induced by the applied immunotherapy. Hence, we subsequently analyzed the samples for clonally expanded T cells. This analysis was extended to cover not only BV5 but also the regions BV8 and BV12, which were highly expressed in some of the tumors. However, the initial approach to test for clonality by direct sequencing of PCR products was hampered by the inherent low sensitivity of this method. Thus, a DGGE-based method was established for the detection of clonotypic TCR transcripts in a murine system. We have recently described the use of DGGE for the detection of clonality in human T cell populations. The sensitivity of this approach enables the detection of clonal transcripts constituting as low as 0.1% of the TCR transcripts in a mixed T cell population (30). As shown in Fig. 3, DGGE analysis of both transfected and nontransfected tumors revealed the presence of clonotypic T cells. These data suggest that the T cells responsible for tumor clearance are recognizing tumor-associated antigens expressed by the parental tumor cells and not antigens induced by the process of transfection. In this regard, the murine analogues of human MART-1, glycoprotein of $M_r$ 100,000, and tyrosinase-related protein 2 were recently cloned from a B16 melanoma cDNA library (31, 32). Furthermore, cytotoxic T cell clones recognizing B16 melanoma, which exert their action in a tumor-specific and major histocompatibility complex-restricted manner, have been raised from C57BL/6 mice (33). These data strongly suggest that clonal T cell responses against melanoma-associated antigens are a general feature of murine B16 melanoma. Although B16 melanoma is generally considered to be a weak or even nonimmunogenic tumor, possibly because of a low expression of major histocompatibility complex class I molecules (34), these reports along with the data presented herein indicate that B16 melanoma fulfills the requirements to elicit a specific major histocompatibility complex-restricted T cell response. Such an immune response could have been boosted by targeted IL-2 therapy of established melanoma metastases. For all three TCRBV regions analyzed, more than one clonal transcript was present; this was most evident in treated tumors (Fig. 3), e.g., BV5 analysis revealed the presence of five to eight different clonal transcripts. This finding predicates that T cell clones are present at levels which are not detectable prior to therapy, but are expanded by IL-2 targeted to the tumor microenvironment by ch14.18–IL-2. These data suggest that the majority of the T cells present in the tumor subsequent to *in situ* IL-2 therapy are tumor specific since their activation is dependent on both antigen recognition and the presence of IL-2. However, at present it is not possible to confirm that the

T cell clones detected *in situ* are directly implicated in the T cell-mediated antitumor immune response induced by targeted IL-2 therapy. Although our knowledge and understanding of tumor-specific T cells have expanded considerably, current *in vitro* analysis may not reflect the *in vivo* immune status because *in vitro* culture steps may introduce major biases (35).

To date, only a limited number of studies have characterized tumor-infiltrating lymphocytes in tumors treated with IL-2 at the molecular level. One of these studies suggested that regression of P815 tumors, induced by intratumoral injection of an adenoviral vector expressing IL-2, was caused by a polyclonal nonspecific T cell population (36). The means for assessing clonality in this study was based on analyzing infiltrating T cells by the ''Immunoscope'' approach (37) which uses CDR3 size as a marker for clonality. Consequently, a T cell clone will be revealed by the presence of a high number of transcripts having the exact same length of CDR3. The inherent problems of this approach are obvious, i.e., a large number of different T cell clones are difficult to distinguish simply by the length of CDR3. In contrast, the DGGE method reveals clonality on the basis of melting properties, meaning that transcripts having the exact same length will be focused at different positions in the gel (30). TCR transcripts of different lengths may, in theory, have similar melting properties and consequently may focus at the same position in a denaturing gradient gel. Sequencing a high number of individual bands has, however, revealed a single sequence in all cases, suggesting that cofocusing of different TCR transcripts is probably a rare event. The discrepancy of the data in these two studies is therefore most likely due to the different methods used. An alternative explanation for this obvious discrepancy between these two studies could be the different means of IL-2 administration.

A successful antitumor T cell response involves induction, recruitment, and effector functions of T cells. The presence of clonotypic T cells in the B16 G3.12 and B78–D14 tumors without any specific therapy suggests that clonally expanded tumor-specific T cells are present in the tumor-infiltrating lymphocyte population prior to therapy with the ch14.18–IL-2 fusion protein; thus, targeted immune therapy seems to be involved in the modulation of later phases of a cellular immune response. Importantly, our results imply that anergized or otherwise inactive T cells can be activated by means of targeted IL-2 therapy without the requirement for specialized antigen-presenting cells or the induction of new or modified peptide antigens.

We thank D. Lützhøft for preparation of tissue samples. This study was supported by grants from the Danish Cancer Society.

1. Boon, T. & van der Bruggen, P. (1996) *J. Exp. Med.* **183,** 725–729.
2. Castelli, C., Rivoltini, L., Mazzocchi, A. & Parmiani, G. (1997) *Int. J. Clin. Lab. Res.* **27,** 103–110.
3. thor Straten, P., Becker, J. C., Seremet, T., Bröcker, E. B. & Zeuthen, J. (1996) *J. Clin. Invest.* **98,** 279–284.
4. Salvi, S., Segalla, F., Rao, S., Arienti, F., Sartori, M., Bratina, G., Caronni, E., Anichini, A., Clemente, C., Parmiani, G. & Sensi, M. (1995) *Cancer Res.* **55,** 3374–3379.
5. Maas, R. A., Dullens, H. F. & Den, O. W. (1993) *Cancer Immunol. Immunother.* **36,** 141–148.
6. Dummer, R., Gore, M. E., Hancock, B. W., Guillou, P. J., Grobben, H. C., Becker, J. C., Oskam, R., Dieleman, J. P. & Burg, G. (1995) *Cancer (Philadelphia)* **75,** 1038–1044.
7. Pardoll, D. M. (1995) *Annu. Rev. Immunol* **13,** 399–415.
8. Gillies, SD, Reilly, E. B., Lo, K. M. & Reisfeld, R. A. (1992) *Proc. Natl. Acad. Sci. USA* **89,** 1428–1432.
9. Becker, J. C., Pancook, J. D., Gillies, SD, Mendelsohn, J. & Reisfeld, R. A. (1996) *Proc. Natl. Acad. Sci. USA* **93,** 2702–2707.
10. Becker, J. C., Varki, N., Pancook, J. D., Gillies, SD, Dreier, T., Furukawa, K. & Reisfeld, R. A. (1996) *J. Exp. Med.* **183,** 2361–2366.
11. Kirkin, A. F., thor Straten, P. & Zeuthen, Z. (1996) *Cancer Immunol. Immunother.* **42,** 203–212.
12. Chomczynski, P. & Sacchi, N. (1987) *Anal. Biochem.* **162,** 156–159.
13. Arden, B., Clark, S. P., Kabelitz, D. & Mak, T. W. (1995) *Immunogenetics* **42,** 501–530.
14. Rychlik, W. & Rhoads, R. E. (1989) *Nucleic Acids Res.* **17,** 8543–8551.
15. Johnston, R. F., Pickett, S. C. & Barker, D. L. (1990) *Electrophoresis* **11,** 355–360.
16. Hoppe, B. L., Conti Tronconi, B. M. & Horton, R. M. (1992) *Biotechniques* **12,** 679–680.
17. Mullis, K. (1991) *PCR Methods Appl.* **1,** 1–14.
18. Lerman, L. S. & Silverstein, K. (1987) *Methods Enzymol.* **155,** 482–501.
19. Guldberg, P. & Güttler, F. (1994) *Nucleic Acids Res.* **22,** 880–881.
20. Stackpole, C. W. (1990) *Invasion Metastasis* **10,** 267–280.
21. Haraguchi, M., Yamashiro, S., Yamamoto, A., Furukawa, K., Takamiya, K., Lloyd, K. O. & Shiku, H. (1994) *Proc. Natl. Acad. Sci. USA* **91,** 10455–10459.
22. Sheffield, V. C., Cox, D. R., Lerman, L. S. & Myers, R. M. (1989) *Proc. Natl. Acad. Sci. USA* **86,** 232–236.
23. Van den Eynde BJ & Boon, T. (1997) *Int. J. Clin. Lab. Res.* **27,** 81–86.
24. Schøller, J., thor Straten, P., Birck, A., Siim, E., Dahlstrom, K., Drzewiecki, K. T. & Zeuthen, J. (1994) *Cancer Immunol. Immunother.* **39,** 239–248.
25. Rosenberg, S. A. (1988) *Immunol. Today* **9,** 58–62.
26. Pancook, J. D., Becker, J. C., Gillies, S. D. & Reisfeld, R. A. (1996) *Cancer Immunol. Immunother.* **42,** 88–92.
27. Xiang, R., Lode, H. N., Dolman, C. S., Dreier, T., Varki, N. M., Qian, X., Lo, K. M., Lan, Y., Super, M., Gillies, S.D. & Reisfeld, R. A. (1997) *Cancer Res.* **57,** 4948–4955.
28. Lode, H. N., Xiang, R., Varki, N. M., Dolman, C. S., Gillies, S. D. & Reisfeld, R. A. (1997) *J. Natl. Cancer Inst.* **89,** 1586–1594.
29. Becker, J. C., Varki, N., Bröcker, E. B. & Reisfeld, R. A. (1996) *J. Invest. Dermatol.* **107,** 627–632.
30. thor Straten, P., Barfoed, A., Seremet, T., Saeterdal, I., Zeuthen, Z. & Guldberg, P. (1998) *Biotechniques*, in press.
31. Zhai, Y., Yang, J. C., Spiess, P., Nishimura, M. I., Overwijk, W. W., Roberts, B., Restifo, N. P. & Rosenberg, S. A. (1997) *J. Immunother.* **20,** 15–25.
32. Bloom, M. B., Perry-Lalley, D., Robbins, P. F., Li, Y., El-Gamil, M., Rosenberg, S. A. & Yang, J. C. (1997) *J. Exp. Med.* **185,** 453–459.
33. Wang, R. & Taniguchi, M. (1995) *J. Immunol.* **154,** 1797–1803.
34. Hara, I., Nguyen, H., Takechi, Y., Gansbacher, B., Chapman, P. B. & Houghton, A. N. (1995) *Int. J. Cancer* **61,** 253–260.
35. Faure, F., Even, J. & Kourilsky, P. (1998) *Crit. Rev. Immunol.* **18,** 77–86.
36. Levraud, J. P., Duffour, M. T., Cordier, L., Perricaudet, M., Haddada, H. & Kourilsky, P. (1997) *J. Immunol.* **158,** 3335–3343.
37. Pannetier, C., Cochet, M., Darche, S., Casrouge, A., Zoller, M. & Kourilsky, P. (1993) *Proc. Natl. Acad. Sci. USA* **90,** 4319–4323.